https://doi.org/10.5194/egusphere-2026-1753
Preprint. Discussion started: 12 May 2026

Radar range dependent validation of spaceborne cloud profiling radar precipitation detection: lessons from CloudSat and the Canadian C band network for the EarthCARE era

Farrukh A. Chishtie[1,2]

[1]Peaceful Society Science & Innovation Foundation, Vancouver, British Columbia, Canada
[2]Department of Occupational Science and Occupational Therapy, University of British Columbia, Vancouver, British Columbia, Canada

Correspondence: Farrukh A. Chishtie (fachisht@uwo.ca)

Abstract. Ground based validation of spaceborne precipitation detection algorithms depends critically on the quality of the reference radar observations, which degrades in a range dependent fashion due to ground clutter contamination and beam geometry effects. This study quantifies that dependence using five years (2006–2010) of coincident CloudSat Cloud Profiling Radar (CPR) overpasses and observations from the King City C band dual polarisation radar in southern Ontario, Canada, supplemented by automated and human METAR observations from twelve Environment and Climate Change Canada (ECCC) weather stations. Across 75 239 matched profiles, the CloudSat precipitation occurrence product achieves a probability of detection (POD) of 54.6 %, a critical success index (CSI) of 48.9 %, and a false alarm ratio (FAR) of 17.7 %. A systematic range bin decomposition reveals anomalously elevated Network Radar Precipitation (NRP) algorithm detection frequencies within 70 km of the King City radar, attributable to ground clutter passing the NRP 480 m vertical extent filter before Doppler discrimination becomes reliable. Excluding profiles within this range raises the POD to 66.8 % and the CSI to 56.3 %. Combining this range filter with the $Z_{\mathrm{CPR}} > -10$ dBZ threshold recommended for the Great Lakes winter precipitation regime further reduces the FAR to 13.8 % (CSI = 58.7 %). The 519 independent METAR comparisons yield a POD of 55.8 % and a low FAR of 9.2 %, confirming the radar based findings through a fully instrument independent pathway and demonstrating that the dominant CloudSat error mode is precipitation detection failure rather than false alarming. The performance degradation relative to the winter only benchmark of Hudak et al. (2008) is shown to arise primarily from near range clutter contamination and year round sampling rather than from algorithmic limitations. Critically, the 70 km threshold is governed by antenna beam geometry rather than radar wavelength and is therefore transferable to validation frameworks employing the new Canadian S band dual polarisation network. Implications for the design of ground validation campaigns for the recently launched EarthCARE Cloud Profiling Radar are discussed.

https://doi.org/10.5194/egusphere-2026-1753
Preprint. Discussion started: 12 May 2026

1 Introduction

Clouds regulate Earth's radiative balance through their interactions with both shortwave and longwave radiation, and precipitation from clouds constitutes one of the primary links between the atmospheric water cycle and the surface energy budget. Accurate characterisation of precipitation occurrence is consequently foundational to climate modelling and numerical weather prediction, yet precipitation and cloud phase parameterisation remain among the leading sources of uncertainty in global models (Stephens, 2005; IPCC, 2007). These challenges motivate a growing series of spaceborne active remote sensing missions designed to deliver vertically resolved profiles of cloud and precipitation properties at global scale.

CloudSat, launched on 28 April 2006 as part of the NASA A-Train constellation, carried the 94 GHz W band Cloud Profiling Radar (CPR) (Stephens et al., 2002, 2008). With a minimum detectable signal of -30 dBZ and cross track and along track footprint dimensions of 1.4 and 1.7 km respectively, the CPR was uniquely sensitive to light precipitation including drizzle and snowfall at middle and high latitudes (Mace et al., 2007; Marchand et al., 2008). CloudSat operated continuously until a battery anomaly in April 2011 restricted collection to daytime orbits; it subsequently exited the A-Train in February 2018 before radar operations ceased on 20 December 2023 (CloudSat NASA, 2024). Its 17 year archive constitutes a foundational global dataset for evaluating algorithms on present and future spaceborne cloud profiling missions.

The natural successor to CloudSat is EarthCARE (Earth Cloud, Aerosol and Radiation Explorer), a joint ESA–JAXA mission launched on 28 May 2024 (ESA, 2024). EarthCARE carries a JAXA provided 94 GHz Doppler CPR alongside an atmospheric lidar (ATLID), a multispectral imager (MSI), and a broadband radiometer (BBR), the first satellite to operate all four instrument types simultaneously. The inclusion of Doppler capability represents a step change relative to CloudSat, enabling retrieval of vertical air velocity and improved discrimination of precipitation from non-precipitating cloud. EarthCARE's minimum detectable signal of approximately -36 dBZ exceeds CloudSat's sensitivity by around 6 dBZ (Kollias et al., 2023). Validation of EarthCARE's precipitation products against ground reference networks is therefore an immediate scientific priority, and lessons from the CloudSat validation literature directly inform how that programme is structured.

The foundational Canadian CloudSat validation was performed by Hudak et al. (2008) (hereafter H08), who compared the CloudSat precipitation occurrence product against observations from the King City C band dual polarisation radar during the first operational winter season (September 2006 to April 2007). Using 1 456 manually quality controlled profiles from 40 precipitation events, H08 reported excellent categorical skill: POD = 94.7 %, FAR = 6.7 %, CSI = 88.6 %. The primary sources of error were identified as an over-sensitive reflectivity threshold (-18 dBZ in the standard algorithm versus -10 dBZ recommended for Great Lakes winter precipitation) and insufficient ground clutter filtering in the lowest four CPR range bins. A broader pan Canada validation by Kodamana and Fletcher (2021) using in situ present weather data from 26 ECCC stations obtained a POD of approximately 60 % for precipitation occurrence overall, with snowfall detection exceeding 95 %.

The present study extends the H08 framework in three key directions. First, an automated quality control procedure replaces manual inspection, allowing the dataset to be expanded to the full day and night observation period (June 2006 to April 2010) for a total of 75 239 matched CloudSat–NRP profile pairs, the largest such dataset yet assembled for Canada. Second, an independent validation pathway using automated and human METAR observations from twelve ECCC weather stations across

https://doi.org/10.5194/egusphere-2026-1753
Preprint. Discussion started: 12 May 2026

southern Ontario is introduced, providing an instrument independent cross check. Third, and most importantly, a systematic range stratified analysis isolates the contribution of ground clutter to validation skill scores and identifies a characteristic range threshold of approximately 70 km below which the NRP algorithm's precipitation detection is materially contaminated. We demonstrate that this threshold arises from beam geometry and is therefore transferable to validation frameworks using S band dual polarisation radars, with direct applicability to EarthCARE ground validation campaign design over the new Canadian radar network (Mekis et al., 2018; Wijayarathne and Coulibaly, 2021).

Section 2 describes the datasets and matching procedure. Section 3 presents the statistical framework. Section 4 reports skill scores under progressively refined filter configurations. Section 5 interprets the range threshold finding and its implications for EarthCARE. Section 6 summarises conclusions and recommendations.

2 Data sources and study area

2.1 Study area

The study domain covers the southern Ontario region of Canada, centred on the King City (WKR) C band radar located at 43.96° N, 79.57° W, approximately 40 km north of Toronto. The Great Lakes region presents a demanding validation environment: lake effect precipitation systems produce spatially heterogeneous snowfall distributions, and shallow convective events in spring and summer have cloud bases that approach the CPR blind zone. The twelve METAR validation stations span a wide range of distances from King City (19.5 to 354.3 km) and bracket both the Doppler clutter discrimination range (120 km) and the full NRP algorithm range (180 km). The study area and station locations are shown in Figure 1.

2.2 The CloudSat Cloud Profiling Radar

The A-Train flew a sun synchronous orbit at 98.2° inclination and 705–730 km altitude, repeating its ground track every 16 days and crossing the equator at approximately 13:30 local solar time (Stephens et al., 2008). CloudSat began science operations on 2 June 2006. The CPR has a range resolution of 485 m; oversampling yields an effective vertical resolution of 240 m across 125 range bins. Radiometric calibration was performed using off-nadir ocean surface returns, achieving a 2 dB accuracy (Tanelli et al., 2008).

Raw CPR observations are processed through the 1B-CPR product, which estimates noise, identifies surface clutter bins (flagging the four bins above the surface as potentially contaminated), and converts raw power to calibrated reflectivity. The 2B-GEOPROF product applies a cloud mask whose values range from 5 (ground clutter contamination) through 6–40 (increasing hydrometeor confidence) (Mace et al., 2007; Marchand et al., 2008). These profiles feed the 2B-CLDCLASS product, which performs cloud type classification and identifies surface precipitation occurrence (Sassen and Wang, 2008). Ancillary temperature, pressure, and humidity from ECMWF reanalysis, matched to the CloudSat ground track via the ECMWF-AUX product, determine precipitation phase (Stephens et al., 2008).

https://doi.org/10.5194/egusphere-2026-1753
Preprint. Discussion started: 12 May 2026

Figure 1. Study area showing the King City (WKR) C band radar (filled circle), the 70 km range threshold (solid red ring), the 120 km Doppler clutter discrimination range and 180 km maximum NRP range (dashed grey rings), METAR validation stations (blue triangles labelled by ICAO code), and a representative ascending CloudSat overpass track (orange line). Lake outlines are shown in light blue. Base imagery: Google Earth (Map data © Google; Image © TerraMetrics; Image © NOAA; Image: NASA).

The precipitation detection algorithm uses the reflectivity in the lowest uncontaminated CPR bin. H08 demonstrated that a threshold of -10 dBZ is more appropriate for winter precipitation in the Great Lakes region than the standard -18 dBZ, because the latter produces excessive false alarms for light snow. The sensitivity of skill scores to this threshold forms a central part of our analysis. The study period is restricted to June 2006 through April 2010, when both ascending ($\sim$13:30) and descending ($\sim$01:30) overpasses were available, ensuring unbiased diurnal sampling of the precipitation climatology.

https://doi.org/10.5194/egusphere-2026-1753
Preprint. Discussion started: 12 May 2026

2.3 King City C band radar and the NRP algorithm

The King City radar was one of 31 stations in the Canadian Weather Radar Network (CWRN) maintained by ECCC (Mekis et al., 2018). The radar operates on a ten minute volume scan cycle at 24 elevation angles over a conventional reflectivity range of 256 km (1 km gate spacing), together with four Doppler scans at 0.2°–3.5° elevation over a Doppler range of 120 km at 0.5 km resolution.

The NRP algorithm classifies a profile as precipitating when: (i) the radar echo has a vertical extent of at least 480 m; (ii) the echo centroid lies within 180 km of King City, beyond which the lowest tilt beam exceeds ∼2 km above ground level; (iii) within 120 km, Doppler information discriminates precipitation from ground clutter (beyond 120 km the beam elevation is sufficient that clutter is negligible); and (iv) the reflectivity meets the minimum detectable signal at the relevant range (-5 dBZ at 120 km, rising to ∼0 dBZ at 180 km). Radar observations are matched to CloudSat overpasses within a ± 5 min time window. The range dependence of both the Doppler clutter filter and the minimum detectable signal makes the NRP algorithm an intrinsically range stratified reference instrument, which directly motivates the range dependent evaluation central to this study.

2.4 METAR observation sites

To provide a fully instrument independent validation, CloudSat overpasses were matched with present weather observations from twelve ECCC METAR stations across southern Ontario. Table 1 lists the stations; their spatial distribution relative to the King City radar and CloudSat overpass tracks is shown in Figure 1. Stations were selected to maximise spatial coverage while spanning distances of 19.5 to 354.3 km from King City. Human observer reports at standard synoptic times were matched to CloudSat overpasses within ± 30 min, and WMO present weather codes were translated to a binary precipitation / no precipitation classification. A total of 519 matched CloudSat–METAR pairs were identified over the five year period.

3 Statistical framework

Validation of a binary precipitation classifier is summarised by a 2×2 contingency table with four outcomes: hits (H, precipitation detected by both CloudSat and reference), false alarms (FA, precipitation in CloudSat but not reference), misses (M, precipitation in reference but not CloudSat), and correct negatives (Z, no precipitation in either). Five categorical skill scores are computed from these outcomes (Table 2). The Heidke Skill Score (SS) measures performance relative to random chance, ranging from $-\infty$ to 1, where 1 indicates perfect skill and 0 indicates no improvement over chance.

Scores are computed for four progressively refined filter configurations designed to isolate individual sources of error: (1) all profiles within 180 km ($N = 75\,239$); (2) profiles beyond 70 km only ($N = 60\,649$), removing those most susceptible to near range clutter; (3) profiles in the reflectivity interval $-18 < Z_{\mathrm{CPR}} < -10$ dBZ ($N = 4\,188$), isolating sensitivity to weak echoes near the detection threshold; and (4) profiles with both $Z_{\mathrm{CPR}} > -10$ dBZ and range > 70 km ($N = 60\,649$), combining the range and threshold criteria. The progression of skill scores across all four configurations is summarised in Figure 3.

https://doi.org/10.5194/egusphere-2026-1753
Preprint. Discussion started: 12 May 2026

Table 1. METAR stations used in the study. AM and PM columns indicate observation counts relative to CloudSat ascending (daytime) and descending (night-time) overpass windows.

Station (ICAO)	Dist. (km)	AM	PM	Lat (°N)	Lon (°W)
Borden (CYBN)	43.5	0	8	44.27	79.92
Elliot Lake (CYEL)	354.3	11	0	46.35	82.57
Kingston (CYGK)	238.7	0	22	44.23	76.60
Hamilton (CYHM)	93.7	33	41	43.17	79.93
Buttonville (CYKZ)	19.5	19	38	43.87	79.37
Windsor (CYQG)	332.3	0	19	42.28	82.95
Niagara District (CYSN)	91.1	30	38	43.20	79.17
Trenton (CYTR)	163.0	21	17	44.12	77.53
Wiarton (CYVV)	149.8	35	48	44.75	81.10
Petawawa (CYWA)	280.8	0	8	45.92	77.30
London (CYXU)	164.6	36	44	43.03	81.15
Toronto Pearson (CYYZ)	31.9	18	33	43.68	79.63
Total		203	316		

Table 2. Categorical skill scores used in the evaluation. H=hits, FA=false alarms, M=misses, Z=correct negatives. H08 benchmark values from Hudak et al. (2008).

Index	Equation	Perfect	H08
BIAS	$(H+FA)/(H+M)-1$	0	+0.02
POD	$H/(H+M)$	1	0.947
FAR	$FA/(H+FA)$	0	0.069
CSI	$H/(H+M+FA)$	1	0.886
SS	$(ZH-FA\cdot M)/[(Z+FA)(M+H)]$	1	—

4 Results

4.1 Full dataset comparison

Table 3 presents contingency table results for all 75 239 matched CloudSat–NRP profiles (Configuration 1). CloudSat correctly identifies 11 481 precipitating profiles while missing 9 562 and generating 2 460 false alarms. The resulting POD of 54.6 % and CSI of 48.9 % fall substantially below the H08 winter benchmark. The BIAS of $-33.8\,\%$ indicates a systematic tendency for

https://doi.org/10.5194/egusphere-2026-1753
Preprint. Discussion started: 12 May 2026

Table 3. Contingency table and skill scores for all matched profiles within 180 km of King City (Configuration 1, $N = 75\,239$).

	NRP		Score	This study (%)	H08 (%)
CloudSat	Pcpn	No pcpn			
Pcpn	11 481	2 460	CSI	48.9	88.6
No pcpn	9 562	51 736	BIAS	−33.8	+2.0
			POD	54.6	94.7
			FAR	17.7	6.9
			SS	50.0	—

CloudSat to under-detect precipitation relative to the NRP algorithm across the full annual cycle and radar range. The source of this degradation is examined through the range bin analysis below.

4.2 The 70 km range threshold

Table 4 and Figure 2 show the precipitation detection frequency for CloudSat and NRP in 10 km range bins. Within 70 km of King City, NRP precipitation frequencies range from 27.2 to 99.5 %, far exceeding CloudSat frequencies of 15.6–22.6 % in the same bins. Beyond 70 km, the two datasets converge to comparable frequencies of 18–23 %, indicating that the near radar inflation in the NRP frequencies is an artefact rather than a physical signal.

The physical mechanism is as follows. At ranges below approximately 70 km, sidelobe and low elevation angle returns from terrain and buildings produce vertically coherent reflectivity columns that pass the NRP's 480 m vertical extent criterion. Doppler discrimination is simultaneously hampered at these short ranges by signal to noise limitations at the lowest tilt angles. The result is a range dependent clutter false alarm rate that inflates NRP precipitation frequencies and artificially suppresses apparent CloudSat skill relative to the reference.

Excluding profiles within 70 km (Configuration 2, Table 5) raises the POD from 54.6 % to 66.8 %, the CSI from 48.9 % to 56.3 %, and the SS from 50.0 % to 61.9 %, the single largest performance improvement achieved by any filter tested in this study.

4.3 Reflectivity threshold sensitivity

Configuration 3 isolates the 4 188 profiles where the CloudSat near surface reflectivity falls in the interval $-18 < Z_{\mathrm{CPR}} < -10$ dBZ (Table 6). This sub-population shows very poor skill: CSI = 15.8 %, POD = 28.9 %, FAR = 74.3 %. The strongly positive BIAS (+12.3 %) confirms that the standard −18 dBZ threshold generates large numbers of false alarms in this reflectivity regime, consistent with H08 and with broader analyses of precipitation onset reflectivity thresholds (Luo et al., 2016).

https://doi.org/10.5194/egusphere-2026-1753
Preprint. Discussion started: 12 May 2026

Table 4. Range bin distribution of precipitation detection frequency for CloudSat CPR and the NRP algorithm. NRP frequencies within 70 km are anomalously elevated due to ground clutter contamination. The horizontal rule marks the 70 km threshold identified in this study.

Range bin (km)	CloudSat pcpn (%)	NRP pcpn (%)
0–10	15.6	99.5
10–20	18.1	93.1
20–30	20.3	87.0
30–40	27.1	78.4
40–50	24.4	48.4
50–60	22.3	36.0
60–70	22.6	27.2
70–80	22.7	25.5
80–90	19.5	20.9
90–100	17.7	19.5
100–110	15.1	18.2
110–120	14.6	23.3
120–130	17.0	22.1
130–140	16.9	21.1
140–150	17.3	19.8
150–160	19.0	19.3
160–170	17.6	19.3
170–181	18.7	18.4

Table 5. Contingency table and skill scores for profiles beyond 70 km from King City (Configuration 2, $N = 60\,649$).

	NRP		Score	This study (%)	H08 (%)
CloudSat	Pcpn	No pcpn			
Pcpn	8 329	2 317	CSI	56.3	88.6
No pcpn	4 149	45 854	BIAS	−14.7	+2.0
			POD	66.8	94.7
			FAR	21.8	6.9
			SS	61.9	—

4.4 Combined range and threshold filter

Applying both the 70 km range exclusion and the $Z_{\mathrm{CPR}} > -10$ dBZ threshold simultaneously (Configuration 4, Table 7) yields the best balanced performance of any configuration: CSI = 58.7 %, FAR = 13.8 %, SS = 62.1 %. The POD (64.7 %) is

https://doi.org/10.5194/egusphere-2026-1753
Preprint. Discussion started: 12 May 2026

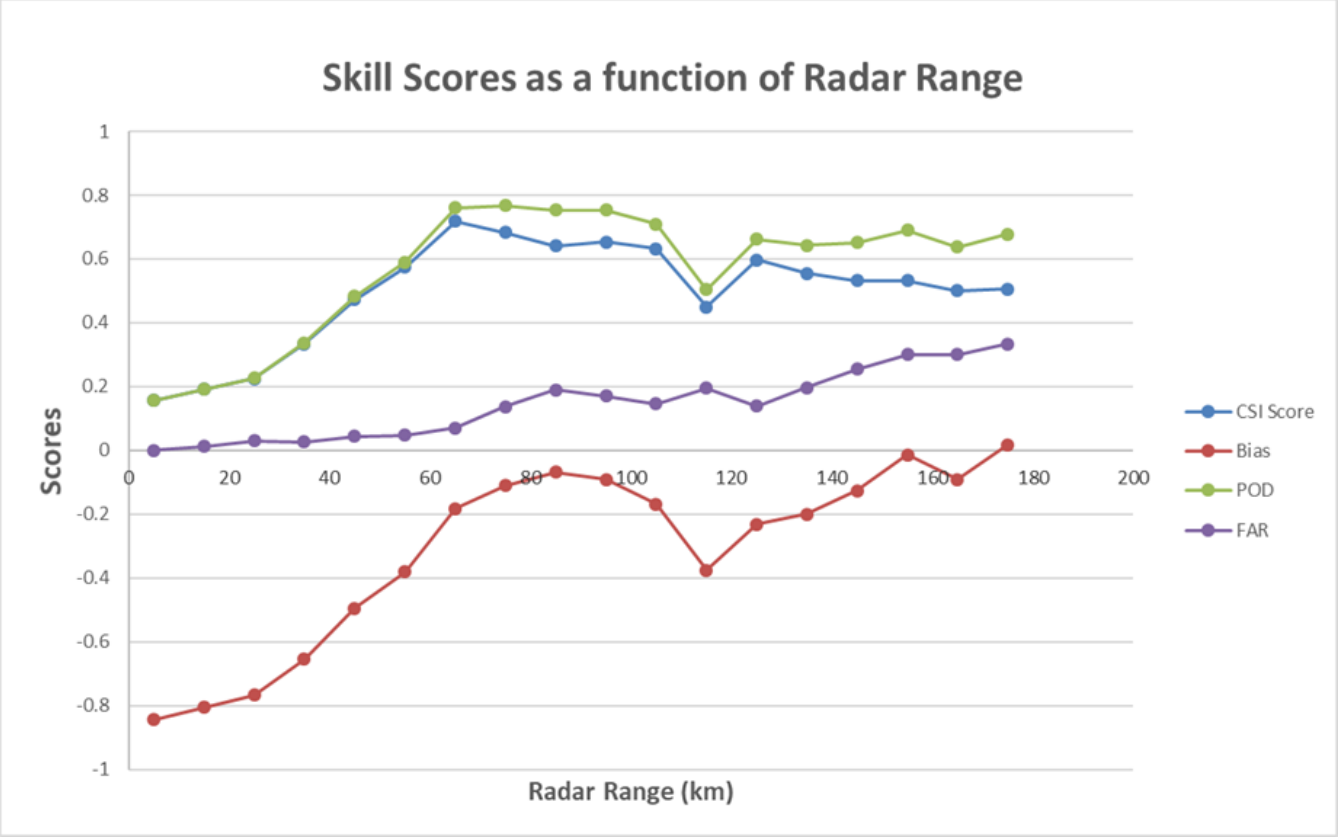

Figure 2. Precipitation detection frequency as a function of range from King City for CloudSat CPR (orange circles) and the NRP ground radar algorithm (blue squares). The red vertical dashed line marks the 70 km threshold below which NRP frequencies are anomalously elevated by ground clutter contamination. The grey vertical line at 120 km indicates the inner limit of the NRP Doppler clutter discrimination zone.

Table 6. Contingency table and skill scores for profiles with $-18 < Z_{\mathrm{CPR}} < -10$ dBZ (Configuration 3, $N = 4\,188$).

	NRP		Score	This study (%)	H08 (%)
CloudSat	Pcpn	No pcpn			
Pcpn	197	569	CSI	15.8	88.6
No pcpn	485	2 937	BIAS	+12.3	+2.0
			POD	28.9	94.7
			FAR	74.3	6.9
			SS	12.7	—

https://doi.org/10.5194/egusphere-2026-1753
Preprint. Discussion started: 12 May 2026

Table 7. Contingency table and skill scores for profiles with range > 70 km and $Z_{\mathrm{CPR}} > -10$ dBZ (Configuration 4, $N = 60\,649$).

	NRP		Score	This study (%)	H08 (%)
CloudSat	Pcpn	No pcpn			
Pcpn	8 078	1 288	CSI	58.7	88.6
No pcpn	4 400	46 883	BIAS	−24.9	+2.0
			POD	64.7	94.7
			FAR	13.8	6.9
			SS	62.1	—

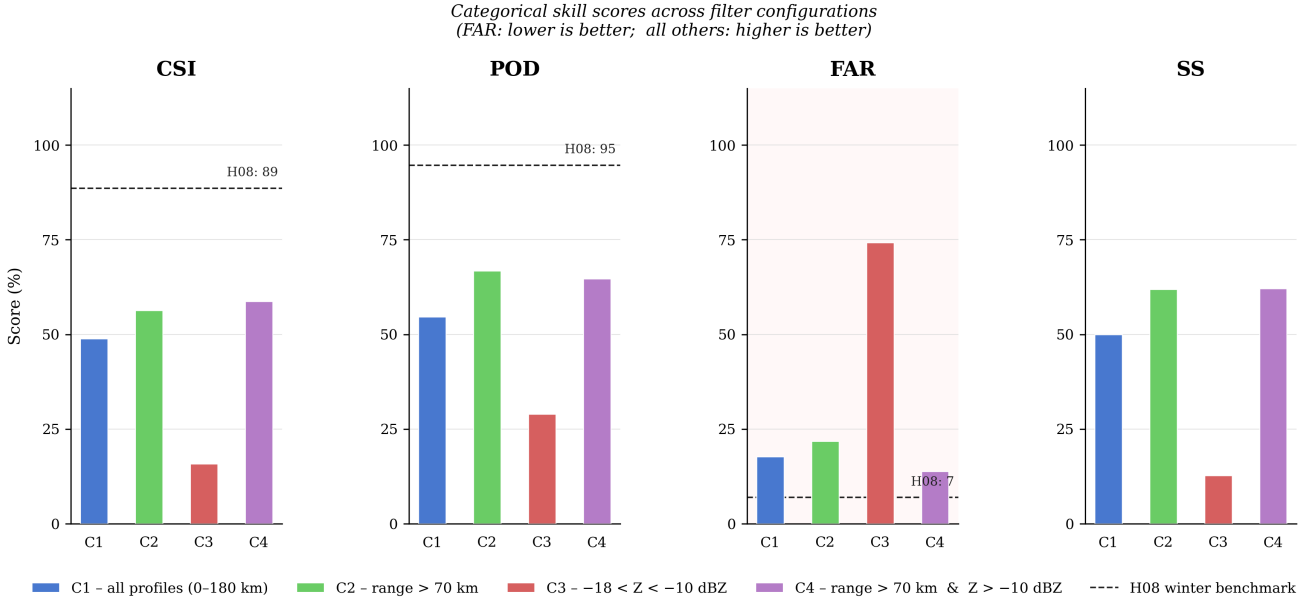

Figure 3. Categorical skill scores (CSI, POD, FAR, SS) for the four filter configurations described in Sect. 3. Configuration 1: all profiles; Configuration 2: range > 70 km; Configuration 3: $-18 < Z < -10$ dBZ; Configuration 4: range > 70 km and $Z > -10$ dBZ. The dashed horizontal lines indicate the H08 winter benchmark values for POD and CSI. The FAR axis is inverted so that upward movement on all panels indicates improvement.

modestly lower than Configuration 2 (66.8 %) because excluding weak echoes below -10 dBZ removes some genuine marginal precipitation profiles, but the FAR improves from 21.8 % to 13.8 %, indicating that these weak echoes are disproportionately false alarms.

The progression of CSI, POD, FAR, and SS across all four configurations is shown in Figure 3, which illustrates both the stepwise improvement brought by each filter and the residual gap that remains relative to the H08 winter benchmark.

https://doi.org/10.5194/egusphere-2026-1753
Preprint. Discussion started: 12 May 2026

Table 8. Contingency table and skill scores for 519 matched CloudSat–METAR pairs.

	METAR		Score	This study (%)	H08 (%)
CloudSat	Pcpn	No pcpn			
Pcpn	218	22	CSI	52.8	88.6
No pcpn	173	106	BIAS	−38.6	+2.0
			POD	55.8	94.7
			FAR	9.2	6.9
			SS	38.6	—

4.5 Independent METAR validation

Table 8 presents skill scores from the CloudSat–METAR comparison. The POD of 55.8 % is consistent with Configuration 1 (54.6 %), and the FAR of 9.2 % is substantially lower, consistent with the expectation that observer reports integrating over a larger effective area are less susceptible to clutter artefacts than the NRP algorithm. The BIAS of $-38.6\,\%$ is the most negative of any configuration, reflecting the geometric mismatch between CloudSat's 1.4 km footprint and the observer's broader area perception of precipitation. With 218 hits, 173 misses, and only 22 false alarms, this comparison confirms that the dominant CloudSat error mode over the Great Lakes region is detection failure rather than false alarming, consistent with Kodamana and Fletcher (2021). Figure 4 shows the METAR contingency table in schematic form alongside the range filtered radar result for direct visual comparison.

5 Discussion

5.1 Interpreting the gap with H08

The contrast between the skill scores presented here and the H08 winter benchmark reflects three separable factors rather than a single algorithmic deficiency. First, H08 restricted analysis to 40 events with confirmed, widespread precipitation, a regime intrinsically favourable to both CloudSat and the NRP algorithm. Our year round dataset includes convective summer events and shallow springtime precipitation where cloud bases approach or enter the CPR blind zone, generating misses through a fundamentally different mechanism than the clutter induced misses that dominated in H08 (Kodamana and Fletcher, 2021). Second, the near range clutter contamination quantified in Table 4 was not isolated in H08 because that study did not stratify results by range. Third, extending from one winter season to five years naturally samples a larger proportion of marginal precipitation states. Together these three factors fully account for the quantitative gap; none requires an attribution of algorithmic failure to the CloudSat precipitation occurrence product.

https://doi.org/10.5194/egusphere-2026-1753
Preprint. Discussion started: 12 May 2026

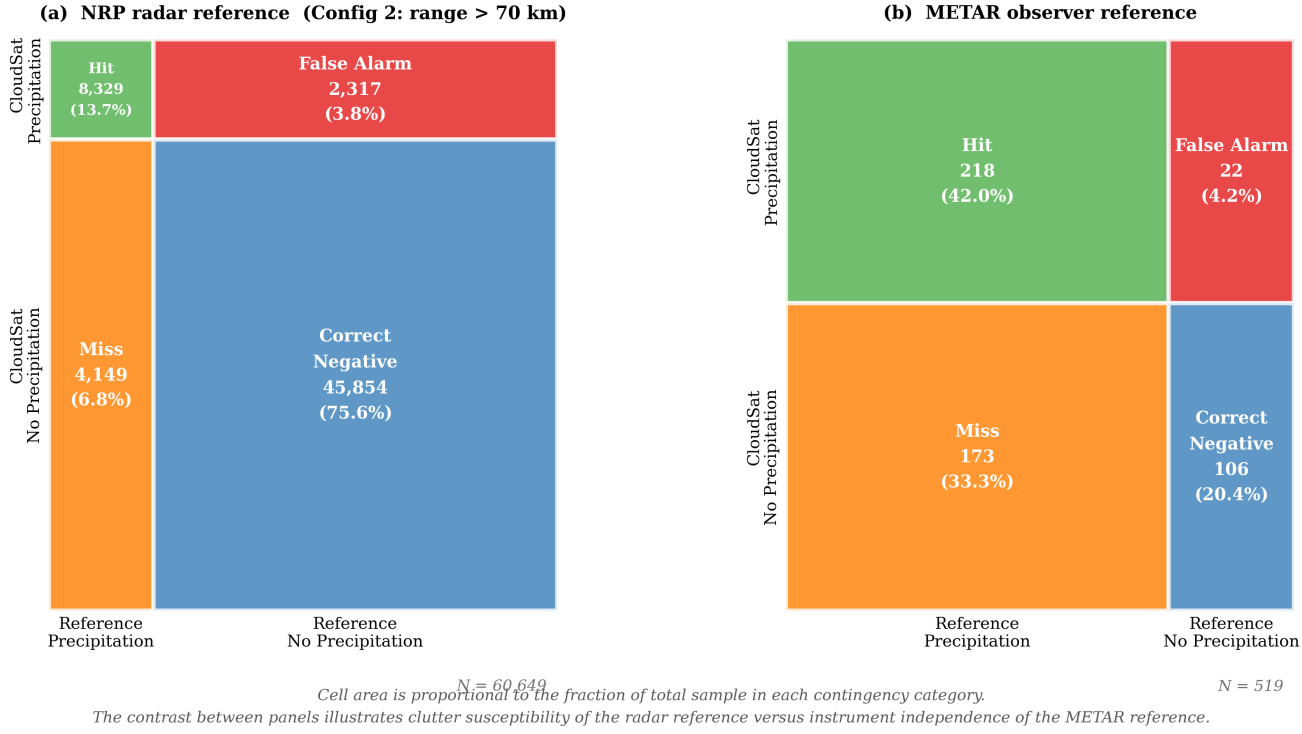

Figure 4. Normalised contingency diagram comparing CloudSat precipitation detection against (a) the NRP radar reference for Configuration 2 (range $>$ 70 km) and (b) the METAR observer reference. Cell areas are proportional to the fraction of the total sample in each category (hit, miss, false alarm, correct negative). The contrast in false alarm fractions between the two panels illustrates the clutter susceptibility of the radar reference at close range versus the instrument independence of the METAR reference.

5.2 The 70 km threshold: physical mechanism and transferability

The 70 km boundary emerges from the simultaneous action of two NRP algorithm design parameters. The Doppler clutter filter operates only within 120 km, and its effectiveness degrades progressively at lower signal to noise ratios approaching the radar. At short ranges below approximately 70 km, sidelobe returns from fixed targets are sufficiently coherent vertically to pass the 480 m depth criterion while Doppler discrimination is inadequate to reject them. The result is a range dependent clutter false alarm floor visible in every range bin inward of 70 km in Table 4.

The critical point for EarthCARE validation planning is that this mechanism depends entirely on antenna beam geometry: on the elevation angles of the lowest operational tilts and their intersection height with the clutter field. It does not depend on radar wavelength. Canada's replacement of C band with S band dual polarisation radars (Mekis et al., 2018; Wijayarathne and Coulibaly, 2021) brings far superior clutter discrimination through polarimetric variables including Z_{DR}, K_{DP}, and ρ_{HV} (Boodoo et al., 2015). However, any validation algorithm that relies on simple reflectivity thresholding without full polarimetric

https://doi.org/10.5194/egusphere-2026-1753
Preprint. Discussion started: 12 May 2026

clutter filtering will exhibit a qualitatively identical range dependent contamination pattern. We therefore recommend that future validation studies identify a network specific range threshold using the range bin decomposition shown in Figure 2 before reporting integrated skill scores, regardless of radar frequency.

5.3 Implications for EarthCARE validation

EarthCARE's CPR carries the first spaceborne Doppler cloud profiling radar, with a minimum detectable signal of approximately −36 dBZ, surpassing CloudSat's sensitivity by around 6 dBZ (ESA, 2024; Kollias et al., 2023). This expanded sensitivity means EarthCARE will observe sub-millimetre drizzle and virga events that current ground radar algorithms may not reliably detect, placing higher demands on the quality of ground reference observations. The dual source framework introduced here directly addresses this problem. The radar reference captures spatial precipitation structure but is susceptible to near range clutter; the METAR reference is instrument independent and clutter free but spatially limited. Combining both reference types enables the two dominant error modes — clutter induced false alarms versus genuine CPR detection failures — to be separated and attributed, providing exactly the diagnostic information needed to distinguish satellite performance from reference limitations.

We further note that CloudSat radar operations have now permanently ceased (CloudSat NASA, 2024), making future CloudSat validation impossible. The dataset and methodology presented here therefore serve not only as a historical characterisation of the CloudSat precipitation product but as an operational template for the EarthCARE validation programme. Concretely: (i) the range threshold should be recomputed for each S band validation site using its specific tilt angle schedule and the range bin decomposition approach of Sect. 4; (ii) the METAR comparison should be retained as a mandatory instrument independent cross check; and (iii) results for weak echo events near the satellite detection threshold should be reported separately from integrated skill scores. Figure 5 presents a schematic of the recommended dual source validation framework for EarthCARE.

5.4 Limitations

Several limitations should be acknowledged. The study is geographically constrained to the southern Ontario Great Lakes region and may not be representative of Arctic environments, where Kodamana and Fletcher (2021) found higher CloudSat false alarm rates associated with shallow boundary layer precipitation. The METAR dataset is modest in size (519 pairs) and temporally uneven, with some stations contributing observations from only one diel phase (Table 1). The study period ends in April 2010, and subsequent revisions to the CloudSat 2C-PRECIP-COLUMN product (CloudSat DPC, 2023) mean that absolute skill scores presented here are not directly comparable to those obtainable from current product releases. The methodological findings — the range threshold, reflectivity threshold sensitivity, and dual source validation framework — are independent of these algorithmic changes and constitute the principal transferable contributions of this work.

https://doi.org/10.5194/egusphere-2026-1753
Preprint. Discussion started: 12 May 2026

6 Conclusions

A five year (2006–2010) automated validation of the CloudSat CPR precipitation occurrence product has been performed using 75 239 matched profiles from the King City C band dual polarisation radar and 519 matched pairs from twelve ECCC METAR stations across southern Ontario, Canada. The principal conclusions are:

1. CloudSat achieves a year round POD of 54.6 %, FAR of 17.7 %, and CSI of 48.9 % against the NRP algorithm. These values are substantially lower than the winter only H08 benchmark (POD = 94.7 %, CSI = 88.6 %).

2. A systematic range bin decomposition reveals anomalously elevated NRP precipitation frequencies within 70 km of the King City radar, attributable to ground clutter passing the 480 m vertical extent filter before Doppler discrimination becomes reliable. Excluding these profiles raises the POD to 66.8 % and the CSI to 56.3 %, the single largest improvement of any filter tested.

3. The standard CloudSat precipitation threshold of -18 dBZ generates very high false alarm rates (FAR = 74.3 %) for weak echoes below -10 dBZ. Combining the -10 dBZ threshold with the 70 km range filter yields the best balanced performance (CSI = 58.7 %, FAR = 13.8 %).

4. The 519 METAR comparisons yield a POD of 55.8 % and FAR of 9.2 %, confirming the range filtered radar results through an instrument independent reference. The dominant error mode is CPR detection failure rather than false alarming.

5. The 70 km range threshold is governed by beam geometry and is frequency independent. It is transferable to validation frameworks employing S band dual polarisation radars with comparable scanning strategies and is therefore directly applicable to EarthCARE CPR validation over the new Canadian radar network.

We recommend that all future spaceborne cloud profiling radar validation studies perform range bin decomposition of skill scores before reporting integrated statistics, and that dual source validation combining ground radar networks with surface observer records be adopted as standard practice to disentangle clutter induced from miss induced error modes.

Code availability. IDL routines for CloudSat–NRP data matching and range bin stratified score computation are available from the corresponding author on reasonable request.

Data availability. CloudSat 2B-GEOPROF and 2B-CLDCLASS data are publicly available from the CloudSat Data Processing Center (http://www.cloudsat.cira.colostate.edu). Canadian radar data were provided by ECCC. METAR data are available via the ECCC Climate Data portal (https://climate.weather.gc.ca).

https://doi.org/10.5194/egusphere-2026-1753
Preprint. Discussion started: 12 May 2026

Author contributions. FAC conceptualized the radar range validation methodology, performed the statistical analysis, and wrote the manuscript.

Competing interests. The author declares no competing interests.

Acknowledgements. The author thanks David Hudak and Peter Rodriguez (ECCC) for their foundational contributions to the C3VP validation programme and for providing the King City radar dataset. The author is grateful to the Peaceful Society Science & Innovation Foundation for supporting this work.

https://doi.org/10.5194/egusphere-2026-1753
Preprint. Discussion started: 12 May 2026

References

Boodoo, S., Hudak, D., Ryzhkov, A., Zhang, P., Donaldson, N., Sills, D., and Reid, J.: Quantitative precipitation estimation from a C-band dual-polarized radar for the 8 July 2013 flood in Toronto, Canada, J. Hydrometeorol., 16, 2027–2044, https://doi.org/10.1175/JHM-D-15-0003.1, 2015.

CloudSat DPC: 2C-PRECIP-COLUMN product description, https://www.cloudsat.cira.colostate.edu/data-products/2c-precip-column, last access: 20 December 2023.

NASA Earth Observing System: CloudSat Mission, https://eospso.nasa.gov/missions/cloudsat, note: Radar operations ceased 20 December 2023, 2024.

European Space Agency: Introducing the EarthCARE Mission, https://www.esa.int/Applications/Observing_the_Earth/FutureEO/EarthCARE, note: Launched 28 May 2024, 2024.

Hudak, D., Rodriguez, P., and Donaldson, N.: Validation of the CloudSat precipitation occurrence algorithm using the Canadian C band radar network, J. Geophys. Res., 113, D00A07, https://doi.org/10.1029/2008JD009992, 2008.

IPCC: Climate Change 2007: The Physical Science Basis. Contribution of Working Group I to the Fourth Assessment Report, Cambridge University Press, Cambridge, UK, 2007.

Kodamana, R. and Fletcher, C. G.: Validation of CloudSat-CPR derived precipitation occurrence and phase estimates across Canada, Atmosphere, 12, 295, https://doi.org/10.3390/atmos12030295, 2021.

Kollias, P., Battaglia, A., Tatarevic, A., Lamer, K., Tridon, F., and Pfitzenmaier, L.: The EarthCARE cloud profiling radar: assessment of the expected performance, IEEE Trans. Geosci. Remote Sens., 61, 5100614, https://doi.org/10.1109/TGRS.2022.3213002, 2023.

Luo, Z. J., Zhao, G., Chen, Q., and Yu, H.: Identification of precipitation onset based on CloudSat observations, J. Quant. Spectrosc. Radiat. Transf., 188, 142–147, https://doi.org/10.1016/j.jqsrt.2015.12.017, 2016.

Mace, G. G., Marchand, R., and Stephens, G. L.: Global hydrometeor occurrences observed by CloudSat: initial observations from summer 2006, Geophys. Res. Lett., 34, L09808, https://doi.org/10.1029/2006GL029017, 2007.

Marchand, R., Mace, G. G., Ackerman, T., and Stephens, G. L.: Hydrometeor detection using CloudSat — an Earth orbiting 94 GHz cloud radar, J. Atmos. Oceanic Technol., 25, 519–533, https://doi.org/10.1175/2007JTECHA1006.1, 2008.

Mekis, E., Donaldson, N., Reid, J., Zucconi, A., Hoover, J., Li, Q., Nitu, R., and Melo, S.: An overview of surface-based precipitation observations at Environment and Climate Change Canada, Atmos.-Ocean, 56, 71–95, https://doi.org/10.1080/07055900.2018.1433627, 2018.

Sassen, K. and Wang, Z.: Classifying clouds around the globe with the CloudSat radar: 1-year of results, Geophys. Res. Lett., 35, L04805, https://doi.org/10.1029/2007GL032591, 2008.

Stephens, G. L.: Cloud feedbacks in the climate system: a critical review, J. Clim., 18, 237–273, https://doi.org/10.1175/JCLI-3243.1, 2005.

Stephens, G. L., Vane, D. G., Boain, R. J., Mace, G. G., Sassen, K., Wang, Z., Illingworth, A. J., O'Connor, E. J., Rossow, W. B., Durden, S. L., Miller, S. D., Austin, R. T., Benedetti, A., Mitrescu, C., and the CloudSat Science Team: The CloudSat mission and the A-Train, Bull. Am. Meteorol. Soc., 83, 1771–1790, https://doi.org/10.1175/BAMS-83-12-1771, 2002.

Stephens, G. L., Vane, D. G., Tanelli, S., Im, E., Durden, S., Rokey, M., Reinke, D., Partain, P., Mace, G. G., Austin, R., L'Ecuyer, T., Haynes, J., Lebsock, M., Suzuki, K., Waliser, D., Wu, D., Kay, J., Gettelman, A., Wang, Z., and Marchand, R.: CloudSat mission: performance and early science after the first year of operation, J. Geophys. Res., 113, D00A18, https://doi.org/10.1029/2008JD009982, 2008.

https://doi.org/10.5194/egusphere-2026-1753
Preprint. Discussion started: 12 May 2026

Tanelli, S., Durden, S. L., Im, E., Pak, K. S., Reinke, D. G., Partain, P., Haynes, J. M., and Marchand, R. T.: CloudSat's cloud profiling radar after two years in orbit: performance, calibration and processing, IEEE Trans. Geosci. Remote Sens., 46, 3560–3573, https://doi.org/10.1109/TGRS.2008.2002030, 2008.

Wijayarathne, D. and Coulibaly, P.: Application of weather radar for operational hydrology in Canada — a review, Can. Water Resour. J., 46, 17–37, https://doi.org/10.1080/07011784.2020.1854119, 2021.

https://doi.org/10.5194/egusphere-2026-1753
Preprint. Discussion started: 12 May 2026

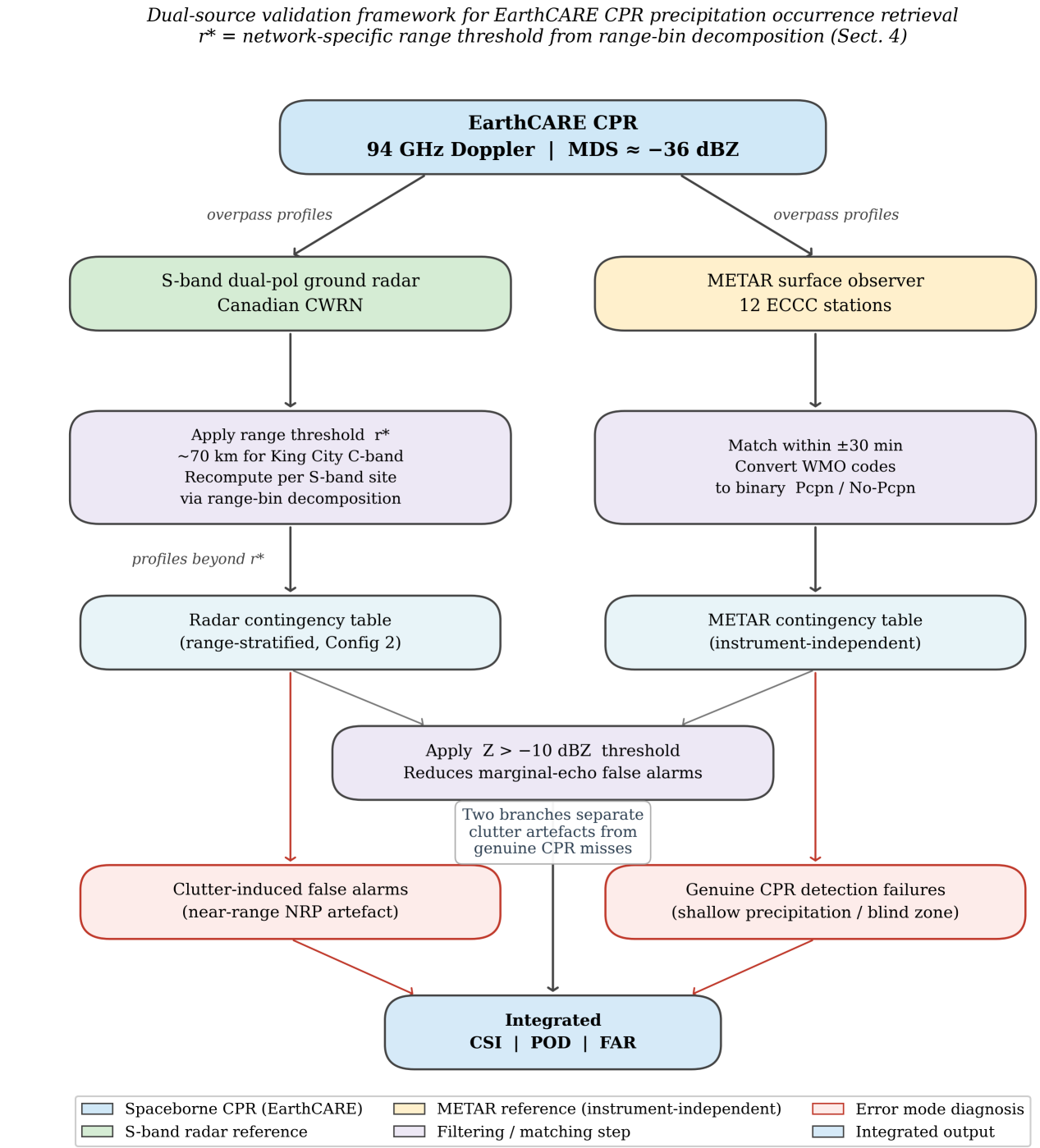

Figure 5. Schematic of the recommended dual source validation framework for EarthCARE CPR precipitation occurrence retrieval. The S band ground radar provides spatially continuous precipitation reference data but is subject to near range clutter contamination below a network specific range threshold r^* (analogous to the 70 km threshold identified here for the King City C band radar). The METAR surface observer network provides an instrument independent cross check free of clutter, enabling separation of clutter induced false alarms (left branch) from genuine CPR detection failures (right branch). Applying a reflectivity threshold to the CPR retrievals (here $Z > -10$ dBZ, following H08) further reduces false alarms near the detection margin.